PROPAGATION MODES OF AURORAL KILOMETRIC RADIATION: A REVIEW

Kozo Hashimoto*

Department of Electrical Engineering, Kyoto University, Sakyo-ku, Kyoto 606

Abstract: *L–O* mode Auroral Kilometric Radiation as well as *R–X* mode AKR are recently observed against the belief of single mode AKR. Observations that contributed to AKR mode determinations are reviewed and recent interpretations of the existence of both modes are introduced. Some observations which claimed *R–X* mode AKR can be interpreted that they consist of both mcde.

1. Introduction

Auroral Kilometric Radiation (AKR) was previously considered to consist of a single mode and was a subject of long controversy, but AKR is now believed to consist of both right-hand polarized extraordinary (*R–X*) and left-hand polarized ordinary (*L–O*) modes. The propagation mode is essential to consider the generation mechanism of AKR. Theories on AKR generation were reviewed by Grabbe (1981). Observations from distant satellites were reviewed by Green (1981) and the ISIS 1 observations near the source region were discussed by Benson (1981). These and many other papers (*e.g.*, Green *et al.*, 1977; Gurnett and Green, 1978; Kaiser *et al.*, 1978; Benson and Calvert, 1979; Calvert, 1981; James, 1980) claimed that the propagation mode of AKR is the *R–X* mode based on their observations. Some papers claimed that is the *L–O* mode (*e.g.*, Benson, 1982, 1984; Oya and Morioka, 1983). In this article we will review these observational results which have contributed to the mode determinations and some interpretations of the coexistence of both modes.

2. *R–X* Mode Observations

Gurnett (1974) suggested in his pioneering work on AKR that AKR is emitted in the *R–X* mode because it is emitted by electrons which rotate around the magnetic field in the right-hand sense. Green *et al.* (1977) presented the observed angular distribution of AKR by using the Hawkeye 1, Imp 6, and Imp 8 satellites. Observed frequencies were 500, 178, 100 and 56.2 kHz. A two-dimensional occurrence frequency diagram of AKR was plotted in a magnetic latitude and magnetic local time plane for each frequency. Statistically, AKR was usually received only above a certain latitude which depends on local time. The lower the wave frequency, the higher the latitudinal limits. They used two-dimensional ray tracing calculations for both *R–X* and *L–O* modes in order to compare them with the observed angular distributions and interpret the polarization and the generation region of AKR. All rays were as-

* Present address: Tokyo Denki University, 2–2, Kanda Nishiki-cho, Chiyoda-ku, Tokyo 101.

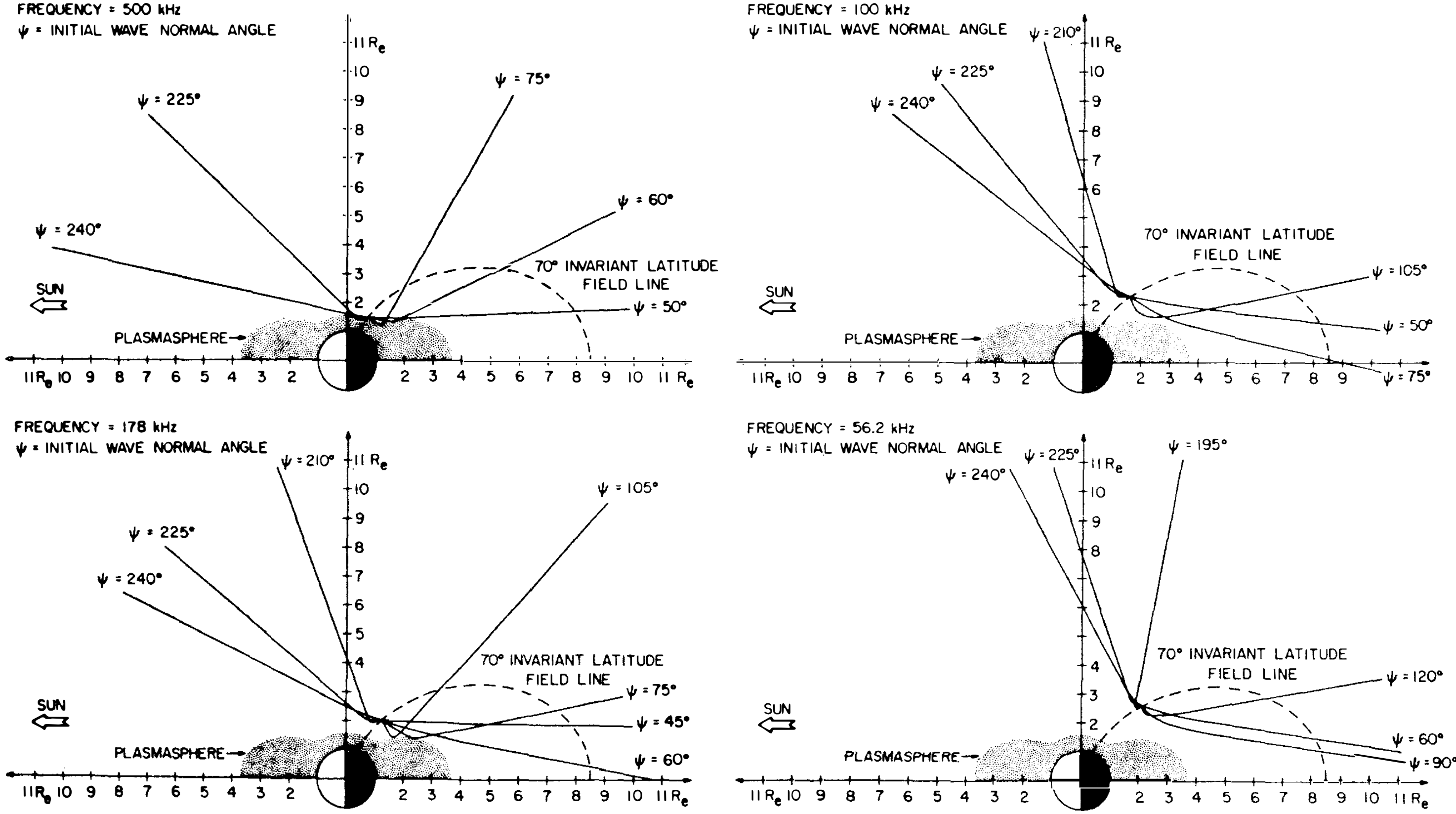

Fig. 1. Ray paths of R–X mode AKR at 500, 178, 100 and 56.2 kHz. The radiation is emitted at all wave normal angles. These paths are consistent with the observed angular distribution (after GREEN *et al., 1977).*

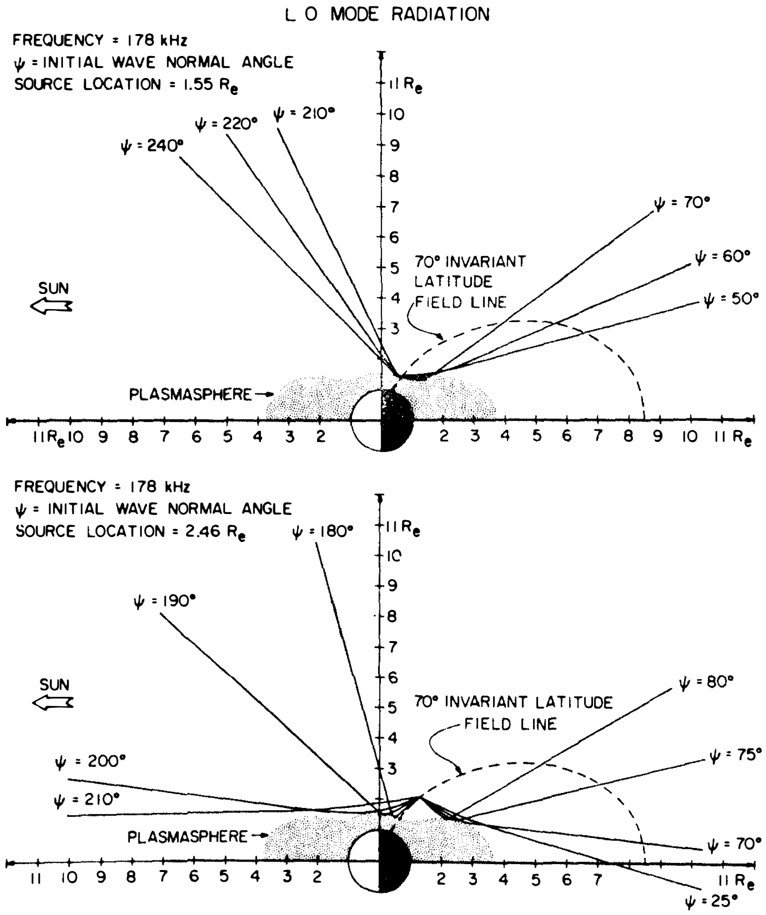

Fig. 2. Ray paths of L–O mode AKR at $f=178$ kHz. The top panel has a source location whose local f_p is close to f and presents rays consistent with the dayside angular distribution. The bottom panel has a source location whose local f_H is close to f and presents rays consistent with the nightside angular distribution (after GREEN *et al., 1977).*

sumed to emanate from a point source at all wave normal directions along a 70° invariant latitude field line. The source altitudes were decided so that a limiting ray direction can agree with the observed dayside or nightside limit for each propagation mode. Figure 1 shows their ray tracing results for the *R–X* mode waves. An initial wave normal angle for a dayside limiting ray, for example, is 240° (in an angle measured clockwise from the upward direction) for each case. The plasmapause affects only ray paths which propagate to the equator in the nightside. The source altitudes for the observed dayside extent are close to those for the nightside extent and a little above the altitudes at which the local *R–X* mode cutoff frequency $f_R[=\sqrt{\{f_p^2+(f_H/2)^2\}}+f_H/2]$ is equal to the wave frequency f. On the other hand, ray paths for *L–O* mode 178 kHz waves are shown in Fig. 2. The bottom panel has a source altitude similar to that of the above case. The nightside rays are also reflected by the plasmapause and latitudinal cutoffs are consistent with the nightside extent of the angular distribution. Rays are hardly refracted near the source. Especially downgoing rays reach very low latitudes in the dayside contrary to the observation. Rays in the top panel have latitudinal cutoffs which are consistent with the observed dayside distribution. Waves propagating toward the dayside must start at a lower altitude so that the wave frequency can be close to the local plasma frequency f_p at the source and L–O mode rays will be refracted more. The source altitudes which account for the dayside and nightside extents are quite different in the case of the L–O mode. As a result, GREEN *et al.* (1977) concluded that AKR is the R–X mode since the R–X mode rays gave the best agreement with the observed angular distribution. It should be noted that the radiation was assumed to be generated over a wide range of wave normal angles and composed of a single mode. These assumptions are not consistent with recent observations.

GURNETT and GREEN (1978) measured low-frequency cutoffs of radio emissions by the Hawkeye 1 satellite at radial distances from about 1.5 to 2.5 R_E (Earth radii) along the auroral field lines (the source region). It was found that all AKR events occurred on the nightside. Figure 3 is a scatter diagram of the power flux of the emissions as a function of a ratio of the wave frequency (178 kHz) to the local cyclotron frequency f_H. Intense auroral hiss emissions are excluded for clarity. AKR events are intense and are observed only if f/f_H is greater than one. Weaker signals which have no cutoff at the local f_H were attributed to continuum radiation. The cutoff at

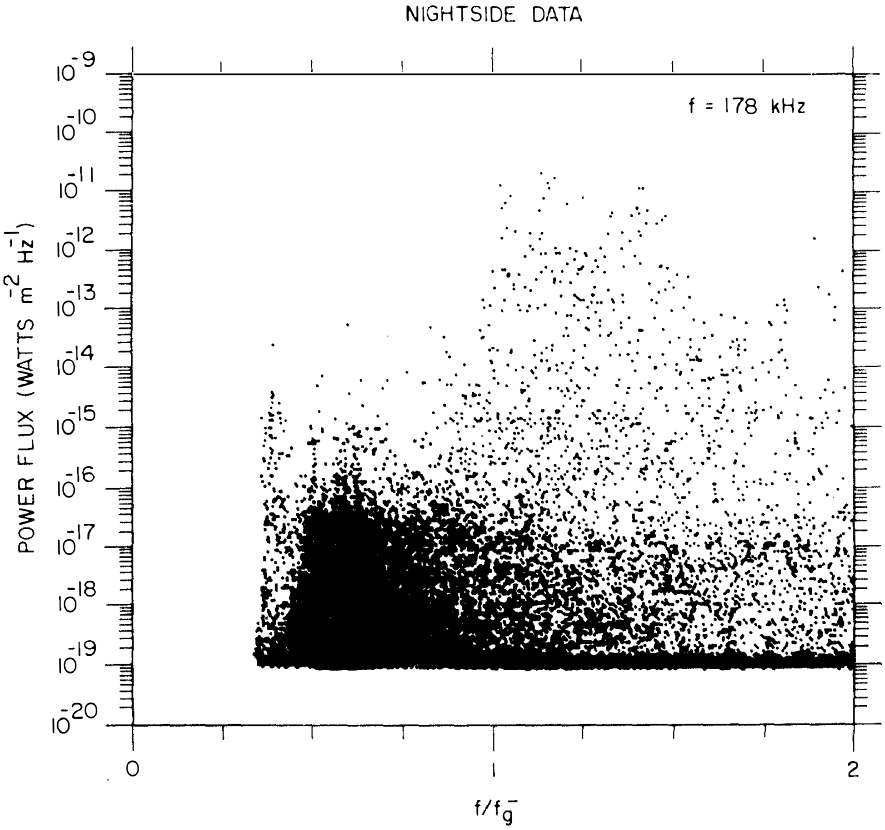

Fig. 3. A scatter diagram of the power flux as a function of f devided by the local f_H received at 178 kHz in the source region by Hawkeye 1. The points at the intense flux are AKR which show sharp cutoff at the local f_H. The points whose intensities are less than 10^{-18} W/(m^2Hz) are due to continuum radiation and shows no cutoff at the local f_H (after GURNETT and GREEN, 1978).

f_H can be interpreted as a propagation effect or a characteristic of the generation mechanism. The former was easier to explain. The cutoff frequency f_H is almost equal to the propagation cutoff frequency of the *R–X* mode because f_p is much less than f_H near the source region. This is convenient for the *R–X* mode AKR. *L–O* mode waves generated downward would produce a f_p cutoff. The *L–O* mode radiation must be generated upward only near the local f_H. GURNETT and GREEN (1978) ruled out a possibility of the *L–O* mode since there was no appropriate theory which met the requirements at that time.

The first direct polarization measurement of AKR was carried out by KAISER *et al.* (1978) from the Planetary Radio Astronomy experiment by the Voyager-1 and -2 spacecraft using the two outputs of a 90° hybrid connected to a pair of orthogonal monopoles. AKR was predominantly Left Hand Circular (LHC). The spacecraft were located on magnetic latitudes higher than 18° in the northern hemisphere. Both LHC and Right Hand Circular (RHC) emissions were exceptionally observed only for one day when Voyager-2 was around 30° in latitude, though the RHC emission was weaker. The LHC polarized AKR was concluded to be *R–X* mode waves from the northern source because the wave vector direction is antiparallel to the geomagnetic field vector there. The LHC and RHC emissions were considered to be both *R–X* mode which independently came from the northern and southern sources, respectively.

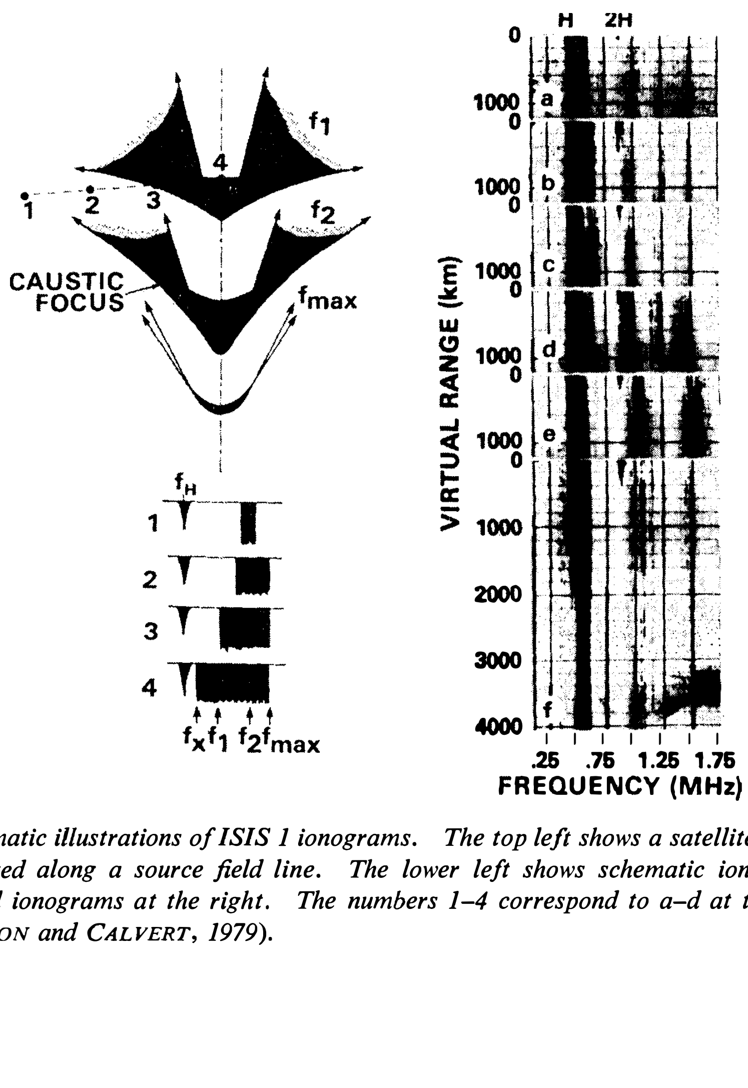

Fig. 4. Schematic illustrations of ISIS 1 ionograms. The top left shows a satellite path and rays radiated along a source field line. The lower left shows schematic ionograms of the actual ionograms at the right. The numbers 1–4 correspond to a–d at the right (after BENSON *and* CALVERT*, 1979).*

Another possibility was that the RHC events were the *L–O* mode from the northern hemisphere.

BENSON and CALVERT (1979) observed AKR by ISIS 1 in the source region. They analyzed changes of the frequency gap between the f_H resonance and the AKR noise band along the satellite path. Figure 4 illustrates analyzed ionograms. The schematic ionograms 1–4 at the lower left correspond to the actual ionograms a–d, respectively. They explained the changes under an assumption that *R–X* mode radiation originated perpendicular to a magnetic field line in an altitude range where the local f_R is slightly less than the wave frequency. The shaded areas of the top left represent the regions where waves generated in the altitude range at the frequencies f_1, f_2 and f_{max} can propagate. The numbers 1–4 along the satellite path correspond to those of the bottom left. The ray originating from the lowest altitude of each area is most refracted because the wave frequency f is closest to f_R. The narrowest gap (number 4) occurs when the satellite is located on the source field line. The gap becomes wider (numbers 3 to 1) as the satellite goes away from the source because only waves emanated from lower altitudes (that is higher frequency) can reach the satellite. CALVERT (1981) confirmed this argument by simplified ray tracing in a constant electron density model. BENSON and CALVERT (1979) and CALVERT (1981) presented clear evidences of *R–X* mode AKR.

JAMES (1980) measured arrival directions of AKR using minima of the spin modulated noise level at 480 kHz received by the dipole of the ISIS 1 sounder receiver. Observed dipole orientations corresponding to the spin minima are shown in Fig. 5.

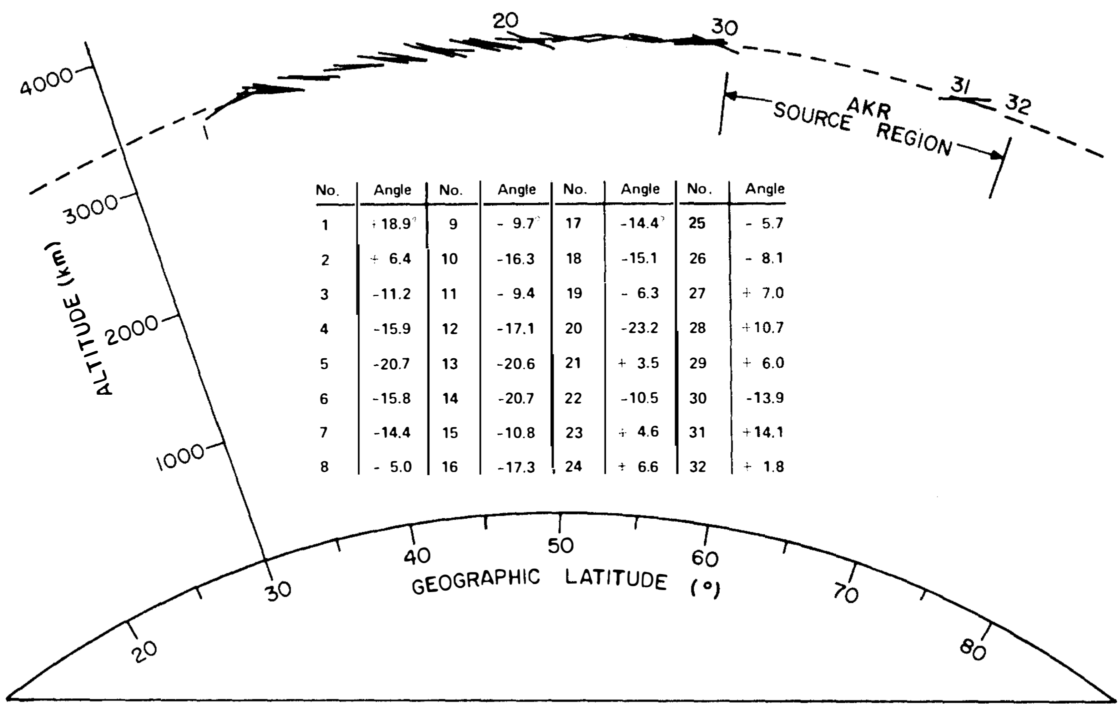

No.	Angle	No.	Angle	No.	Angle	No.	Angle
1	+18.9	9	- 9.7	17	-14.4	25	- 5.7
2	+ 6.4	10	-16.3	18	-15.1	26	- 8.1
3	-11.2	11	- 9.4	19	- 6.3	27	+ 7.0
4	-15.9	12	-17.1	20	-23.2	28	+10.7
5	-20.7	13	-20.6	21	+ 3.5	29	+ 6.0
6	-15.8	14	-20.7	22	-10.5	30	-13.9
7	-14.4	15	-10.8	23	+ 4.6	31	+14.1
8	- 5.0	16	-17.3	24	+ 6.6	32	+ 1.8

Fig. 5. Dipole orientations (the short line segments) derived from spin minima of AKR level at 480 kHz observed by the ISIS 1 topside sounder. The broken line is the satellite trajectory. The numbers above the line segments correspond to those of the table which shows angles between the dipole direction and the horizontal direction (after JAMES*, 1980).*

The angle between the dipole axis and the horizontal direction are listed in the table. Using wave normal directions calculated from these angles, *R–X* mode rays were traced back to the source region. The results showed that wave normal angles were predominantly downward and from about 60° to 90° at 3500 km altitude around the source region. The highest source altitude was higher than 5000 km. A range of f/f_H is so large in the source region. He made no ray tracing for the *L–O* mode.

SHAWHAN and GURNETT (1982) made direct polarization measurements of AKR based on the phase difference between outputs of two dipoles parallel and perpendicular to the spin axis by the DE-1 satellite. They measured the polarization of auroral hiss and AKR, and concluded that both have the same polarization, the *R–X* mode. They also suggested the presence of weaker radiation (weaker by 35 dB or so) of the *L–O* mode taking the departure from the ideal results of the phase difference into account, although the deperture might be due to a calibration bias.

3. *L–O* Mode Observations

OYA and MORIOKA (1983) observed AKR spectra by the Jikiken satellite in a low latitude region (less than 40° in geomagnetic latitudes). They estimated plasma parameters assuming that the upper- and lower-edge frequencies of upper hybrid noise correspond to the upper hybrid frequency and the plasma frequency. The spectra showed cutoff at the local Z mode cutoff frequency, $f_Z[=\sqrt{\{f_p^2+(f_H/2)^2\}}-f_H/2]$ but no cutoff at the local f_R. They concluded that the spectra were composed of escaping *L–O* mode AKR and Z mode waves. The above observations were made near or inside the plasmapause. They interpreted the observations as an evidence of mode conversion of Z mode wave to *L–O* mode AKR based on OYA's (1974) theory.

BENSON (1982, 1984) presented examples of *L–O* mode AKR. Observed AKR bands existed between the f_H resonance and f_R measured by the topside-sounder where local f_p/f_H is greater than 0.3. These were identified as the *L–O* mode because the frequencies in the bands were lower than the cutoff frequency of the *R–X* mode. The *L–O* mode AKR was weaker than the *R–X* mode AKR and was observed near but outside of the source region for the *R–X* mode AKR. Harmonic bands of AKR were also detected.

4. Recent Theories and Interpretations

Several authors have contributed to prove the existence of both modes of AKR. Some radiation mechanisms of AKR, for example, proposed by WU and LEE (1979), can radiate both modes although one mode is stronger than the other. CALVERT (1982) proposed a feedback model which gave sufficient wave growth by multiple partial wave reflections at the source boundaries like a laser. *L–O* mode emissions could be produced by the polarization mismatch at the boundary. OYA and MORIOKA (1983) have some doubts about mode determinations by some observations referred to in Section 2 and show their interpretation on these observations without conflict with their Z and *L–O* mode observations. Realistic ray tracing is required to make sure their ideas. MELROSE *et al.* (1984) evaluated a product of the spatial growth rates

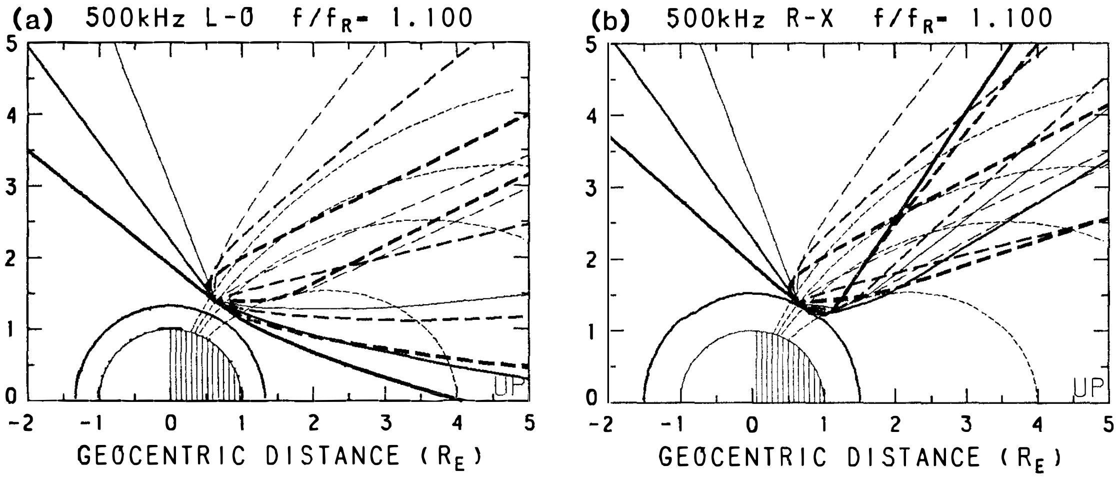

Fig. 6. (a) Ray paths for the L–O mode and (b) for the R–X mode. 500 kHz waves are radiated upward at $f/f_R = 1.1$ along a field line of 70° invariant latitude. The solid lines are ray path propagating in the source meridian plane and the dashed lines are plots of altitudes and latitudes of the waves radiated to off-meridional directions. The thin, medium and thick lines correspond to the initial wave normal angles of 60°, 75° and 90°, respectively. Thin dashed lines threading the earth are field lines of 60°, 67°, 70° and 73° invariant latitudes. The 60° field line represents a plasmapause position. The semicircle around 1.3 or 1.5 shows propagation cutoff of each mode (after HASHIMOTO, 1984).

and the bandwidths of the growing waves (the number of e-folding growths) based on WU and LEE's (1979) loss-cone-driven maser mechanism. They showed the *Z* mode dominates if f_p/f_H is greater than 0.3 and interpreted BENSON's (1984) results as the *Z* mode.

HASHIMOTO (1984) performed three-dimensional ray tracing of AKR for both modes. Examples of ray paths at 500 kHz for the *L–O* and the *R–X* modes are shown in Figs. 6a and 6b, respectively. At the source point $f/f_R = 1.1$ is assumed. Both modes are assumed to be emitted only upward from a single source and their frequencies are assumed to be just above the local f_R. These assumptions are consistent with the requirement for the *L–O* mode given by GURNETT and GREEN (1978) and WU and LEE's (1979) maser mechanism. *L–O* mode coverage of Fig. 6a is consistent with the observed angular distribution (GREEN *et al.*, 1977). It was interpreted that AKR is composed of both modes and the limits of the distribution are decided by the *L–O* mode rays. It was required for the *R–X* mode to be dominant; namely the *R–X* mode should be radiated stronger than the *L–O* mode at the source. Both mode AKR can reach Voyager observation areas (KAISER *et al.*, 1978) in the source hemisphere, although *R–X* mode AKR cannot reach the other hemisphere. He claimed that the Voyager spacecraft must have received weaker *L–O* components as well as stronger *R–X* components. Source points of both modes are not necessarily the same because a small difference of the source points would only slightly change the results. He tried to explain JAMES' (1980) results (see Fig. 5) by the *L–O* mode. Figure 6a indicates that only *L–O* mode waves can be received in a low latitude region.

5. Summary

Observations and interpretations of both modes of AKR are reviewed. It is clarified that indirect mode determinations (GREEN *et al*., 1977; GURNETT and GREEN, 1978) include some doubts in their assumptions. ISIS 1 observations near the source region revealed R–X mode AKR in depletion regions (BENSON and CALVERT, 1979) and L–O mode AKR in relatively dense regions (BENSON, 1982, 1984). The latter could be interpreted as the Z mode (MELROSE *et al*., 1984). Jikiken observations presented clear evidences of L–O mode AKR in a relatively low latitude region (OYA and MORIOKA, 1983). An interpretation of the existence of both modes is proposed by HASHIMOTO (1984). Further observations of angular distributions near and far from the source with clear identification of polarizations and intensities will clarify the real situation.

Acknowledgments

The author would like to thank Prof. I. KIMURA for his useful advice and careful reading of the manuscript.

References

BENSON, R. F. (1981): Auroral kilometric radiation source region observations from ISIS 1. Physics of Auroral Arc Formation, ed. by S.-I. AKASOFU and J. R. KAN. Washington, D. C., Am. Geophys. Union, 369–379 (Geophysical Monograph 25).

BENSON, R. F. (1982): Harmonic auroral kilometric radiation of natural origin. Geophys. Res. Lett., **9**, 1120–1123.

BENSON, R. F. (1984): Ordinary mode auroral kilometric radiation, with hramonics, observed by ISIS 1. Radio Sci., **19**, 543–550.

BENSON, R. F. and CALVERT, W. (1979): ISIS 1 observations at the source of auroral kilometric radiation. Geophys. Res. Lett., **6**, 479–482.

CALVERT, W. (1981): The signature of auroral kilometric radiation on ISIS 1 ionograms. J. Geophys. Res., **86**, 76–82.

CALVERT, W. (1982): A feedback model for the source of auroral kilometric radiation. J. Geophys. Res., **87**, 8199–8214.

GRABBE, C. L. (1981): Auroral kilometric radiation; A theoretical review. Rev. Geophys. Space Phys., **19**, 627–633.

GREEN, J. L. (1981): Observations pertaining to the generation of auroral kilometric radiation. Physics of Auroral Arc Formation, ed. by S.-I. AKASOFU and J. R. KAN. Washington, D. C., Am. Geophys. Union, 359–368 (Geophysical Monograph 25).

GREEN, J. L., GURNETT, D. A. and SHAWHAN, S. D. (1977): The angular distribution of auroral kilometric radiation. J. Geophys. Res., **82**, 1825–1838.

GURNETT, D. A. (1974): The earth as a radio source; Terrestrial kilometric radiation. J. Geophys. Res., **79**, 4227–4238.

GURNETT, D. A. and GREEN, J. L. (1978): On the polarization and origin of auroral kilometric radiation. J. Geophys. Res., **83**, 689–696.

HASHIMOTO, K. (1984): A reconciliation of propagation modes of auroral kilometric radiation. J. Geophys. Res., **89**, 7459–7466.

JAMES, H. G. (1980): Direction-of-arrival measurements of auroral kilometric radiation and associated ELF data from Isis 1. J. Geophys. Res., **85**, 3367–3375.

KAISER, M. L., ALEXANDER, J. K., RIDDLE, A. C., PEARCE, J. B. and WARWICK, J. W. (1978): Direct measurements by Voyagers 1 and 2 of the polarization of terrestrial kilometric radiation. Geophys. Res. Lett., **5**, 857–860.

MELROSE, D. B., HEWITT, R. G. and DULK, G. A. (1984): Electron-cyclotron maser emission; Relative growth and damping rates for different modes and harmonics. J. Geophys. Res., **89**, 897–904.

OYA, H. (1974): Origin of Jovian decametric wave emissions—Conversion from the electron cyclotron plasma wave to the *O*-mode electromagnetic wave. Planet. Space Sci., **22**, 687–708.

OYA, H. and MORIOKA, A. (1983): Observational evidence of *Z* and *L–O* mode waves as the origin of auroral kilometric radiation from the Jikiken (EXOS-B) satellite. J. Geophys. Res., **88**, 6189–6203.

SHAWHAN, S. D. and GURNETT, D. A. (1982): Polarization measurements of auroral kilometric radiation by Dynamics Explorer-1. Geophys. Res. Lett., **9**, 913–916.

WU, C. S. and LEE, L. C. (1979): A theory of the terrestrial kilometric radiation. Astrophys. J., **230**, 621–626.

(*Received May 8, 1984; Revised manuscript received January 4, 1985*)